Original Article

Asian Pacific Journal of Tropical Biomedicine

apjtb.org

doi: 10.4103/apjtb.apjtb_696_24

Zinc oxide nanoparticles synthesized with *Berberis vulgaris* L. ameliorate cyclophosphamide−induced nephrotoxicity in rats

Reza Mohammadian[1], Nader Goodarzi[2✉], Mohsen Akbaribazm[3], Hadi Cheraghi[4]

[1]*Faculty of Veterinary Medicine, Razi University, Kermanshah, Iran*

[2]*Department of Basic Sciences and Pathobiology, Faculty of Veterinary Medicine, Razi University, Kermanshah, Iran*

[3]*Department of Basic Medical Sciences, Khoy University of Medical Sciences, Khoy, Iran*

[4]*Department of Clinical Sciences, Faculty of Veterinary Medicine, Razi University, Kermanshah, Iran*

ABSTRACT

Objective: To examine the protective effects of green-synthesized zinc oxide nanoparticles with *Berberis vulgaris* L. fruit aqueous extract (BVZnONPs) on cyclophosphamide (CP)-induced nephrotoxicity in Wistar rats.

Methods: 35 Adult male Wistar rats were divided into 5 groups: normal, BVZnONPs (20 mg/kg), CP (100 mg/kg), and 2 co-treatment groups receiving CP with BVZnONPs (10 and 20 mg/kg). All treatments were administered intraperitoneally for 28 days. Serum levels of antioxidant enzymes (catalase, superoxide dismutase, glutathione peroxidase, nitric oxide) and kidney function parameters (creatinine, total protein, blood urea nitrogen) were measured. The expressions of p53 and Bcl-2 proteins were assessed *via* immunohistochemical assay while kidney volume and substructures were estimated stereologically.

Results: CP induced nephrotoxicity with significant increases (P<0.05) in nitric oxide, creatinine, and blood urea nitrogen levels, and decreases (P<0.05) in catalase, superoxide dismutase, and glutathione peroxidase levels. It also increased p53 protein expression and decreased Bcl-2 protein expression. Treatment with BVZnONPs significantly increased (P<0.05) antioxidant enzyme levels and decreased nitric oxide levels in the 20 mg/kg group compared to CP. Blood urea nitrogen and creatinine levels were significantly reduced in the BVZnONPs-treated groups, with greater effects at 20 mg/kg. However, total protein serum levels were not significant (P>0.05) in the BVZnONPs-treated groups compared to CP.

Conclusions: These findings suggest that BVZnONPs can mitigate CP-induced nephrotoxicity, likely due to their antioxidant and anti-apoptotic properties, though longer treatment duration may be necessary for tissue-level improvements.

KEYWORDS: Nanoparticle; *Berberis vulgaris* L; Barberry; Kidney; Zinc oxide; Chemotherapy

1. Introduction

The kidneys are essential organs that play a key role in maintaining overall body homeostasis through their ability to filter blood to remove waste, regulate fluid and electrolyte balance, maintain acid-base balance, control blood pressure, produce erythropoietin to produce red blood cells and assist in detoxification. When glomerular filtration rate rapidly declines due to prerenal, intrinsic,

Summary

Question: Do zinc oxide nanoparticles synthesized with *Berberis vulgaris* L. (BVZnONPs) have protective effects on cyclophosphamide-induced nephrotoxicity?

Findings: BVZnONPs could effectively improve antioxidant enzymes, and renal stereology and decrease apoptotic alterations following cyclophosphamide-induced injuries.

Meaning: BVZnONPs have antioxidant and anti-apoptotic effects against cyclophosphamide-induced nephrotoxicity.

✉To whom correspondence may be addressed. E-mail: n.goodarzi@razi.ac.ir

How to cite this article: Mohammadian R, Goodarzi N, Akbaribazm M, Cheraghi H. Zinc oxide nanoparticles synthesized with *Berberis vulgaris* L. ameliorate cyclophosphamide-induced nephrotoxicity in rats. Asian Pac J Trop Biomed 2025; 15(4): 158-168.

Article history: Received 18 November 2024; Revision 17 December 2024; Accepted 15 April 2025; Available online 25 April 2025

or postrenal causes, acute renal disease (also known as acute kidney injury) occurs, causing symptoms such as decreased urine output, swelling, and elevated blood pressure[1]. Fatigue, swelling, high blood pressure, anemia, and electrolyte imbalances are some of the symptoms of chronic renal disease (CKD), which is a progressive loss of kidney function that occurs over months to years and is frequently brought on by diabetes, hypertension, glomerulonephritis, polycystic kidney disease, or chronic obstructive uropathy. Both acute kidney injury and CKD are diagnosed and treated with blood and urine testing, imaging, and addressing underlying causes. Treatment for CKD also includes lifestyle modifications, medicine, and, in more advanced stages, dialysis or transplantation. Continuous research and medical improvements are necessary to better understand these disorders in order to detect them early, manage them effectively, and improve patient outcomes[2]. Cyclophosphamide (CP), methotrexate, and cisplatin are examples of chemotherapy-induced nephrotoxicity that can result in acute kidney injury or CKD by oxidative stress, inflammation, vascular injury, and direct tubular cell destruction[3]. Electrolyte abnormalities such as hyponatremia, hyperkalemia, hypocalcemia, hyperphosphatemia, hypomagnesemia, and hyperuricemia, as well as increased blood urea nitrogen (BUN) and serum creatinine (Cr) levels, are examples of biochemical alterations. Increased reactive oxygen species (ROS), pro-inflammatory cytokines [TNF-α, interleukins (IL-1β and IL-6)], transforming growth factor-beta (TGF-β), apoptosis markers (Bax, p53, and caspase-3), fibrotic markers (fibronectin, collagen I, and α-smooth muscle actin), and renal injury molecules (kidney injury molecule-1, neutrophil gelatinase-associated lipocalin, and cystatin C) are among the molecular alterations[4]. Tubular cell necrosis and apoptosis, mitochondrial malfunction, endothelial damage, inflammatory cell infiltration, and fibrosis are examples of cellular alterations. These intricate changes underscore the necessity of nephrotoxicity prevention and management techniques for chemotherapy patients[5].

Although CP was licensed in 1959 and is widely used to treat severe autoimmune illnesses and a variety of malignancies, it is also known to have nephrotoxic effects. These consequences are typified by structural kidney alterations that affect renal architecture and function, including glomerular injury, tubular necrosis, interstitial fibrosis, and vascular damage[6]. In terms of function, CP lowers glomerular filtration rate, results in electrolyte abnormalities, and causes proteinuria. Inflammatory reactions involving immune cell infiltration and the release of cytokines (such as TNF-α, IL-1, and IL-6) are involved in nephrotoxicity. Depletion of antioxidant enzymes [such as glutathione peroxidase (GPx), superoxide dismutase (SOD), and catalase (CAT)] and an increase in ROS are indicators of oxidative stress from CP.

CP also induces apoptosis *via* mitochondrial pathways, characterized by the upregulation of pro-apoptotic proteins such as Bax and p53, alongside the activation of caspases, which ultimately results in the death of renal cells[7]. Beyond its effects on tumor cells, CP activates separate apoptotic pathways within normal host cells, including renal parenchymal cells. Studies indicate that CP promotes apoptosis in these cells by increasing the expression of apoptotic protease-activating factor 1 (Apaf-1) and caspase-9. Additionally, CP treatment enhances the expression of p27, leading to cell cycle arrest and subsequent apoptosis in renal parenchymal cells. The activation of mitogen-activated protein kinase (MAPK) signaling pathways, including MAPK/ERK kinase 1/2 (MEK1/2) and extracellular signal-regulated kinase 1/2 (ERK1/2), due to chemotherapy agents, significantly affects cell proliferation, survival, and apoptosis[8]. Moreover, CP drugs can alter the expression levels of cyclin D1, leading to its reduction. This alteration in the cell cycle progression subsequently enhances the process of apoptosis in renal parenchymal cells. Grasping these intricate mechanisms is essential for formulating strategies to reduce nephrotoxicity caused by CP[9].

Berberis vulgaris L. (BV), also known as European barberry, is a deciduous shrub indigenous to Europe, Northwest Africa, and Western Asia, reaching heights of up to 4 meters. Its spiny branches bear yellow flowers arranged in drooping racemes, and it produces red oval berries that ripen in late summer and autumn. Rich in phytochemicals, BV's primary alkaloid is berberine, accompanied by other compounds such as berbamine, oxyacanthine, and various flavonoids (including kaempferol, daidzein, genistein, catechin, and quercetin), along with phenolic acids and tannins[10]. Known for its antimicrobial, anti-inflammatory, antioxidant, and anticancer effects, berberine plays a significant role in the regulation of glucose metabolism and lipid profiles. Traditionally utilized across the world for medicinal purposes, BV is employed to treat digestive issues, infections, fevers, and skin ailments. Berberine derived from BV shows potential in suppressing cancer cell growth, promoting apoptosis, and inhibiting angiogenesis in various cancers, including breast, prostate, colorectal cancers, and leukemia. Furthermore, it presents hepatoprotective benefits and cardiovascular advantages by lowering cholesterol levels and preventing atherosclerosis and shows promise in diabetes management and protecting kidneys from nephrotoxicity[11]. Flavonoids found in BV inhibit the activation of NF-κB, which is a key regulator of inflammation, while also suppressing inflammatory enzymes such as COX-2 and iNOS during chemotherapy[12]. The green synthesis of nanoparticles using BV extracts offers environmental advantages by reducing the use of harmful chemicals and leveraging sustainable, biocompatible plant extracts, thereby minimizing ecological impact. The cost-efficiency of BV extracts facilitates accessible nanoparticle production, resulting in biocompatible nanoparticles that are well-suited for biomedical applications such as drug delivery and imaging, while also retaining BV's antioxidant and antimicrobial effects that aid in wound healing and controlling infections[13]. Green synthesis techniques enable precise regulation of nanoparticle properties, improving their effectiveness in catalysis, sensors, and biomedical technologies, and enhancing their stability in aqueous solutions for both biological and environmental purposes. These nanoparticles can be easily modified during the synthesis process, providing specificity in drug delivery across various fields, including medicine, agriculture, and electronics, demonstrating their adaptability and sustainable contributions to modern technology[14].

In this study, our objective was to examine the potential protective and therapeutic effects of zinc oxide nanoparticles synthesized with BV fruit (BVZnONPs) on CP-induced nephrotoxicity in rats. We employed biochemical, immunohistochemical, and histopathological approaches to assess the impact of BVZnONPs on CP-induced nephrotoxicity.

2. Materials and methods

2.1. Preparation of BVZnONPs

To prepare the aqueous extract of BV fruit, 10 g fresh barberry fruit was soaked in 2 L distilled water for 72 h stirring every 8 h using a glass stirrer. The extract was then filtered using Whatman No. 2 paper. Subsequently, 100 mL of the barberry extract was heated in a beaker to 60 ℃, and 5 g zinc nitrate salt was added. The mixture was centrifuged at 400 rpm on a heater stirrer for 30 min until it formed a paste. The resulting paste was then dried in an oven at 120 ℃ for 15 min. The dried powder was pulverized and subjected to centrifugation three times at 2 000 rpm for 5 min each to purify it.

2.2. Physicochemical properties of the BVZnONPs

Various analytical techniques were employed to characterize the BVZnONPs, such as shape, particle size, fractal dimensions, crystallinity, and surface area. Fourier-transform infrared spectroscopy (FTIR) was used to identify the biomolecules associated with the BVZnONPs, covering a range of 400-4 000/cm using a KBr disc (Shimadzu IR Affinity-1). Additionally, dynamic light scattering (DLS), zeta potential (ZP), and field emission scanning electron microscopy (FE-SEM) analyses were conducted using a JEOL 200 kV instrument, with samples placed on a carbon-coated copper grid[14].

2.3. Experimental design

To conduct this study, 35 adult male Wistar rats, approximately 13 weeks old and weighing between 200-250 g, were prepared from Kermanshah University of Medical Sciences. They were kept for one week under laboratory conditions with a temperature of (20 ± 2) ℃, a relative humidity of (45±3)%, and a 12:12 light-dark cycle to acclimate to the environmental and climatic conditions. All rats were kept in compliance with international standard guidelines, protocols, and ethical regulations set forth by the Razi University Ethics Committee (approval no: IR.RAZI.REC.1402.059). After acclimation, the rats were weighed and divided randomly into 5 groups as follows:

The normal group received 1 mL of distilled water intraperitoneally (*i.p.*) for 28 d; the CP group was administered 100 mg/kg of CP *i.p.* on days 1, 10, and 20; the co-treatment groups (CP + BVZnONPs) received CP *i.p.* on days 1, 10, and 20, along with 10 and 20 mg/kg BVZnONPs *i.p.* for 28 d; the BVZnONPs alone group was administered with 20 mg/kg BVZnONPs *i.p.* for 28 d.

LD_{50} technique was used to select the effective dose of non-toxic treatment along with the pilot study and similar studies conducted on CP and BVZnONPs. In this study, administration of CP and BVZnONPs was done during specific and fixed hours, 9 am and 3 pm, respectively[15].

2.3.1. Serum levels of BUN, total protein (TP), and Cr

At the end of the study, the rats were euthanized using a combination of 50 mg/kg xylazine (2%) and 30 mg/kg ketamine (10%) for anesthesia. Blood was collected from the heart, and serum samples were separated using a centrifuge. Serum levels of BUN, Cr, and TP were then measured using a commercial auto-analyzer[16].

2.3.2. GPx, SOD, CAT, and NO serum activity

To measure serum levels of GPx, SOD, CAT, and NO activity, a commercial auto-analyzer was used according to the manufacturer's instructions[16].

2.4. Morphometric and stereological studies

The harvested kidney samples were fixed in 10% formalin solution for 72 h. Since in parenchymatous tissues, the volume of each cubic centimeter is considered equal to 1 g, therefore, in this study, the total volume of kidneys was considered equal to their weight[17].

To calculate the fractional volume of the renal structures, a point probe consisting of 100 pluses (+) with equal distances in the X and Y axes and a light microscope (Olympus CX2, Janan) connected to a camera (KECAM. 5 MP) were used. The points located on each structure (cortex, medulla, glomerulus, proximal and distal convoluted tubules, Henle, and collecting ducts) were counted in each field of view and placed in the following formula to calculate the fractional volume of each structure:

$V_v = \sum P \text{ structure} / \sum P \text{ reference}$

where $\sum P$ structure is the number of points that collided with the desired structure and $\sum P$ reference is the number of points that collided with the reference volume.

Finally, to calculate the total volume of each structure [cortex (CoV), medulla (MeV), proximal convoluted tubule (PCTV), distal convoluted tubule (DCTV), Henle loop (HLV), collecting duct (CDV), and glomerulus volume (GV)], the relative volume of each structure was multiplied by the reference volume[18].

V total (Structure/reference) = V_v (structure/reference) × V reference

where V_v is the relative volume of each structure and V reference is the kidney total volume.

2.5. Kidney histopathology

To evaluate the level of tissue destruction and histopathological changes of the kidney in different groups, the kidneys were fixed in 10% formalin, and 5 µm sections were prepared through tissue preparation and stained with hematoxylin & eosin method. Using an optical microscope (Olympus CX2) connected to a camera (KECAM. 5 MP) system, kidney tissue cortex, and medulla structures were evaluated with 40×, 100×, and 400× magnifications[19].

2.6. Immunohistochemical evaluation of kidney tissues

The slides (5 µm thick sections) were placed in a microwave with a 1× TBS solution (catalog no. T5912, Sigma, US) for 10 min at 100 ℃, and the samples remained in the solution for 20 min. The samples were washed with PBS (catalog no. P4417, Sigma, US) in three steps, each with a 5-minute interval. Next, H_2O_2 (catalog no. 7722-84-1, Sigma, US) was mixed with methanol in a 1:9 ratio and applied to the samples for 10 min at 25 ℃. The samples were washed with PBS, and the primary antibodies [p53 (catalog no. ab238069) and Bcl-2 (catalog no. ab59348) (Abcam, US)], diluted (1:100) with PBS, were added to the samples and incubated at 25 ℃ for 60 min. After this, the samples were washed three times with PBS, each for 5 min. Then, 100 µL of the linker (catalog no. D1000PVP, Diagnostic BioSystems, US) was added to the samples for 15 min. The samples were again washed three times with PBS, and 100 µL of the polymer solution (catalog no. D1000PVP, Diagnostic BioSystems, US) was added to the samples for 30 min. The samples were washed with PBS once more, followed by the addition of 100 µL of the DAB solution (catalog no. ScyTek-ACV999, ScyTek, US) to the samples. After 5 min, the samples were washed with water and then immersed in a hematoxylin stain for 1 min. Subsequently, the samples were washed with water again. After dehydration and clearing, coverslips were mounted on the samples, and they were photographed using an optical microscope (Olympus CX2) connected to a camera (KECAM. 5 MP) system[20].

2.7. Renal scintigraphy

The SPECT radionuclide imaging was performed using a dual-headed small-animal SPECT scanner (HiReSPECT) at the Preclinical Core Facility (TPCF) based at Tehran University of Medical Sciences. Rats were injected *via* the tail vein with about 2 mCi of the labeled Tc-99m DMSA under general anesthesia. One hour after injection, the planar images were collected in a 38×80 matrix and analyzed qualitatively.

2.8. Statistical analysis

Quantitative data were reported as mean ± SD. Statistical analysis of the data was conducted using SPSS software version 16 (IBM Inc, US). The Kolmogorov-Smirnov test was used to assess data normality, with $P>0.05$ considered indicative of normally distributed data. To evaluate differences between group means, a one-way ANOVA test and the Tukey *post hoc* test were employed. A *P*-value of < 0.05 was considered the criterion for statistical significance between the groups tested. GraphPad Prism version 8.1 (GraphPad Inc, US) was used to create the graphs.

3. Results

3.1. Physicochemical properties of BVZnONPs

The results of physical and chemical characteristics of BVZnONPs are presented in Figure 1. According to the results, the zeta potential was measured at –27.3 mV, and the average diameter of the nanoparticles was 187.2 nm (Figure 1).

3.2. Serum levels of Cr, TP, and BUN

The evaluation of serum indicators of kidney function showed that CP significantly increased ($P<0.05$) the serum levels of BUN and Cr compared to the normal group. The serum level of TP showed a decrease compared to the control group, but this decrease was not significant ($P>0.05$). Administration of a 20 mg/kg dose of barberry nanoparticles in the CP-treated group led to a significant ($P<0.05$) decrease in BUN and Cr levels compared to the CP group. The 10 mg/kg dose of barberry nanoparticles in the group co-treated with CP resulted in a significant ($P<0.05$) decrease in serum Cr levels compared to the CP group. Although BUN levels also decreased in this group compared to the CP group, the decrease was not significant ($P>0.05$). The evaluation of the TP serum level showed that while there was an increase in TP levels in the groups treated with barberry nanoparticles (BVZnONPs) compared to the CP group, this increase was not significant ($P>0.05$) (Figure 2). The results were comparable between the normal group and the only BVZnONPs group.

3.3. NO serum levels and serum activity of CAT, GPx, and SOD

The results showed that CP significantly increased ($P<0.05$) the serum level of NO compared to the normal group. The serum levels of GPx, SOD, and CAT enzymes were significantly decreased in the CP group compared to the normal group ($P<0.05$). In the co-treatment group of CP+10 mg/kg BVZnONPs, an increase in the serum levels of NO, GPx and CAT enzymes was observed, but this increase was not significant compared to the CP group ($P>0.05$).

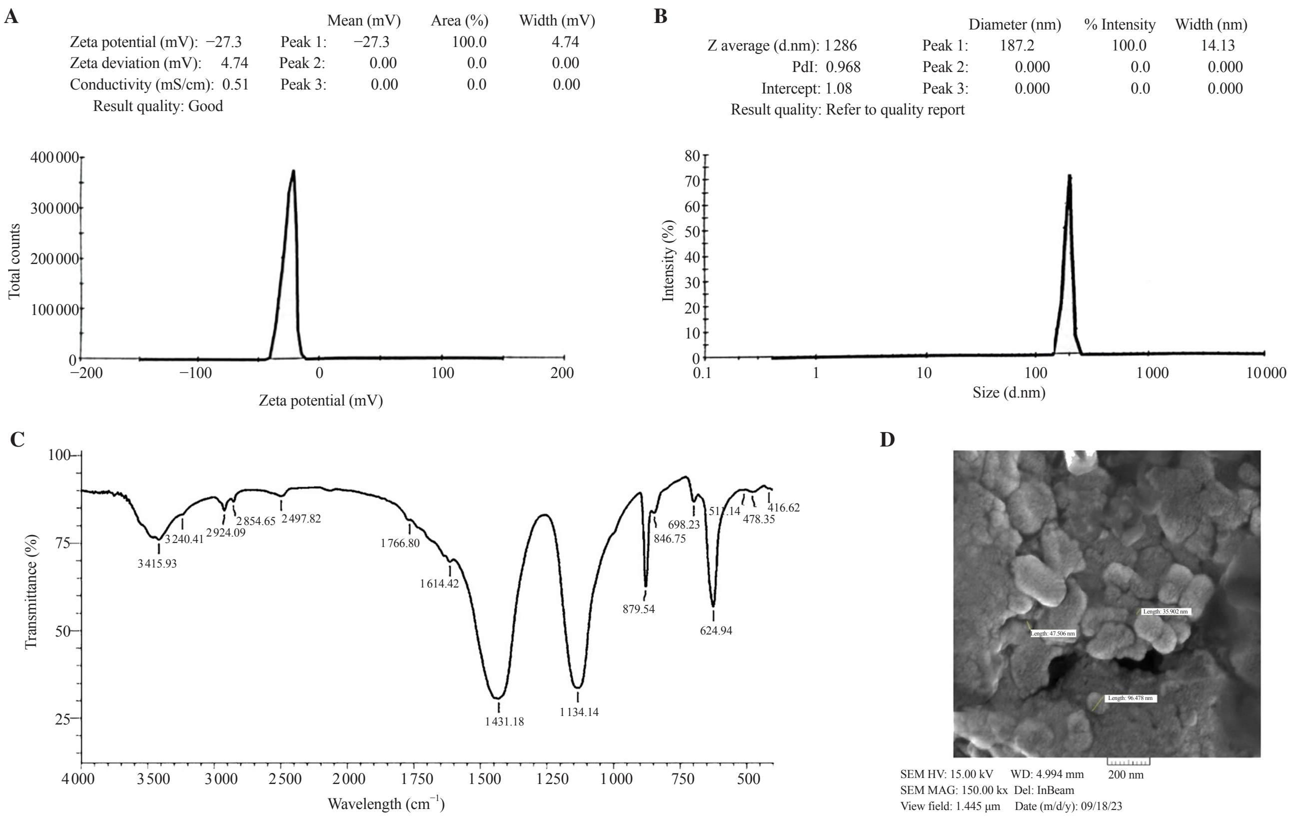

Figure 1. Chemical characterization of zinc oxide nanoparticles with *Berberis vulgaris* L. fruit aqueous extract (BVZnONPs): (A) Zeta potential analysis, (B) Dynamic Light Scattering, (C) Fourier transform infrared spectroscopy (FTIR), and (D) scanning electronic micrograph of BVZnONPs.

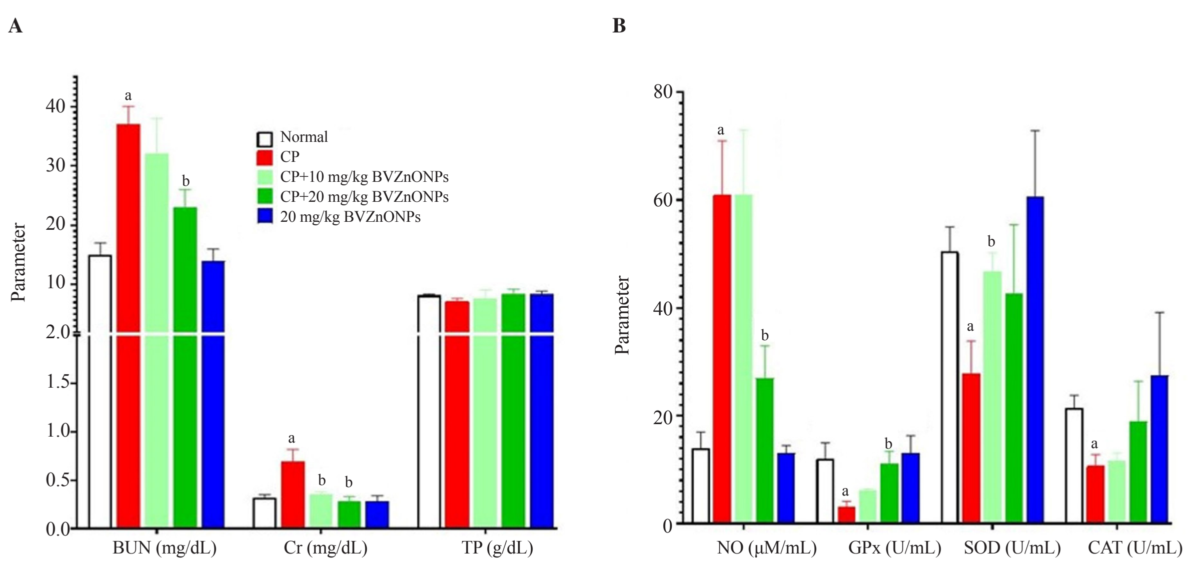

Figure 2. Serum levels of kidney function indicators and antioxidants in experimental groups (mean ± SD; n=6/group). BUN: blood urea nitrogen; Cr: serum creatinine; TP: total protein; NO: nitric oxide; GPx: glutathione peroxidase; SOD: superoxide dismutase; CAT: catalase. [a]$P<0.05$ *vs.* the normal group; [b]$P<0.05$ *vs.* the cyclophosphamide (CP) group.

SOD activity was significantly enhanced by treatment with 10 mg/kg BVZnONPs. In the CP+20 mg/kg BVZnONPs group, there was a significant increase ($P<0.05$) in GPx levels compared to the CP group. In the co-treatment groups (CP+BVZnONPs), the increase in CAT was not significant ($P>0.05$). A significant decrease ($P<0.05$) in NO was observed in the CP+20 mg/kg BVZnONPs group compared to the CP group (Figure 2). The results were comparable between the normal group and the only BVZnONPs group.

3.4. Kidney stereological parameters

The results of stereological measurements of kidneys showed that kidney volume, CoV, MeV, PCTV, GV, HLV, and CDV were significantly decreased ($P<0.05$) in the CP group compared to the normal group, while DCTV showed a slight increase ($P>0.05$) in the CP group. The kidney volume, MeV, and HLV in the treatment groups (CP+10 mg/kg and 20 mg/kg BVZnONPs) showed a

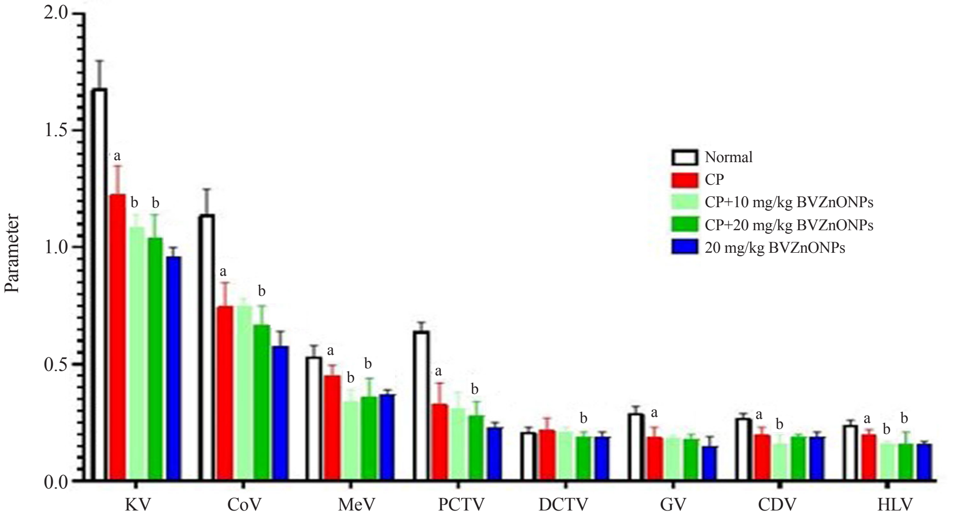

Figure 3. Kidney stereological parameters in experimental groups (means ± SD; n=6/group). $^aP<0.05$ *vs.* the normal group; $^bP<0.05$ *vs.* the CP group. KV: kidney volume; CoV: cortex volume; MeV: medulla volume; PCTV: proximal convoluted tubule volume; DCTV: distal convoluted tubule volume; HLV: Henle loop volume: CDV: collecting duct volume; GV: glomerulus volume.

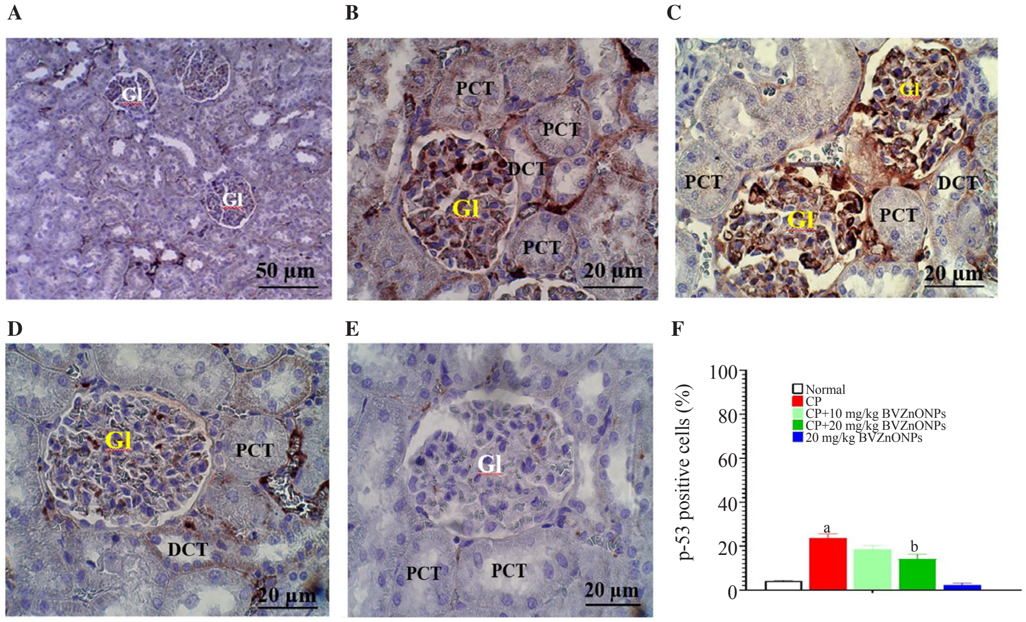

Figure 4. Immunohistochemical staining of p53 in experimental groups: (A) the normal group, (B) the CP group, (C) CP + 10 mg/kg BVZnONPs, (D) CP + 20 mg/kg BVZnONPs, and (E) the 20 mg/kg BVZnONPs group. (F) Quantitative analysis of p53 positive cells in the control and experimental groups. $^aP<0.05$ *vs.* the normal group; $^bP<0.05$ *vs.* the CP group. Gl: glomerulus; PCT: proximal convoluted tubule; DCT: distal convoluted tubule.

significant decrease (P<0.05) compared to the CP group. Also, the CoV and PCTV in the CP+ 20 mg/kg BVZnONPs groups showed a significant decrease (P<0.05) compared to the CP group. The volume of the CDV in the CP+10 mg/kg BVZnONP group had a significant decrease (P<0.05) compared to the CP group (Figure 3).

3.5. Expression of p53 and Bcl-2 proteins

The results showed that in the normal group and the BVZnONPs group, the expression of p53 was very low, while in the CP group, the expression was increased significantly (P<0.05) in the cortex and medulla, especially in the glomeruli compared to the normal group. In the experimental groups treated with CP and 10 mg/kg of BVZnONPs, p53 expression did not show a noticeable decrease, especially in glomeruli. However, in the group treated with CP and 20 mg/kg BVZnONPs, the expression was decreased significantly (P<0.05). The result also showed that in the normal group, the staining intensity of Bcl-2 was high in the urinary tubes and glomeruli, but in the CP group, the expression was reduced significantly (P<0.05) compared to the normal group, especially in the urinary tubes. In the group treated with CP and 20 mg/kg BVZnONPs, the level of Bcl-2 expression showed a significant (P<0.05) increase compared to the CP group, especially in the collecting tubules in the medulla of the kidney (Figures 4 and 5).

3.6. Kidney histopathological results

The renal tissue in the normal group exhibited a normal appearance

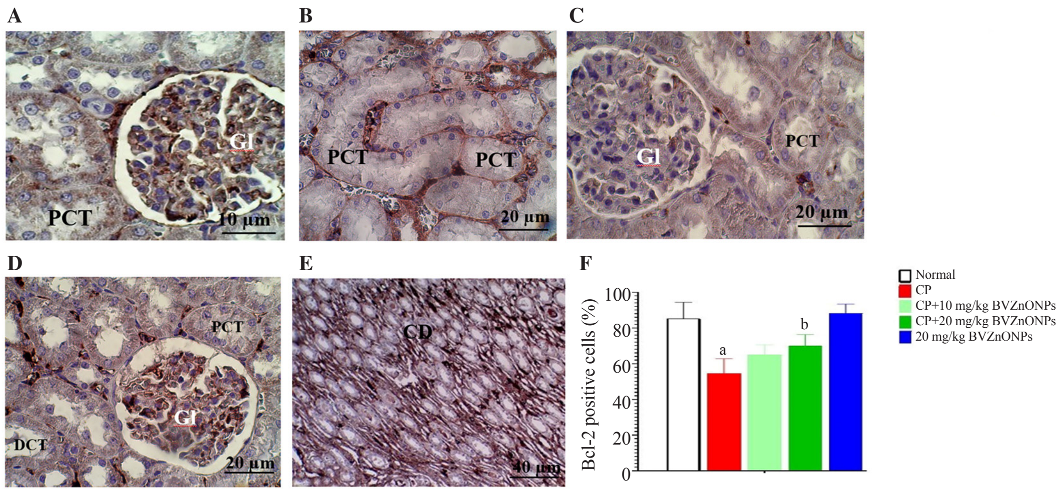

Figure 5. Immunohistochemical staining of Bcl-2 in experimental groups: (A) the normal group, (B) the CP group, (C) CP + 10 mg/kg BVZnONPs, (D) CP + 20 mg/kg BVZnONPs, and (E) the 20 mg/kg BVZnONPs group. (F) Quantitative analysis of Bcl-2 positive cells in the control and experimental groups. [a]P<0.05 *vs.* the normal group; [b]P<0.05 *vs.* the CP group. CD: collecting duct.

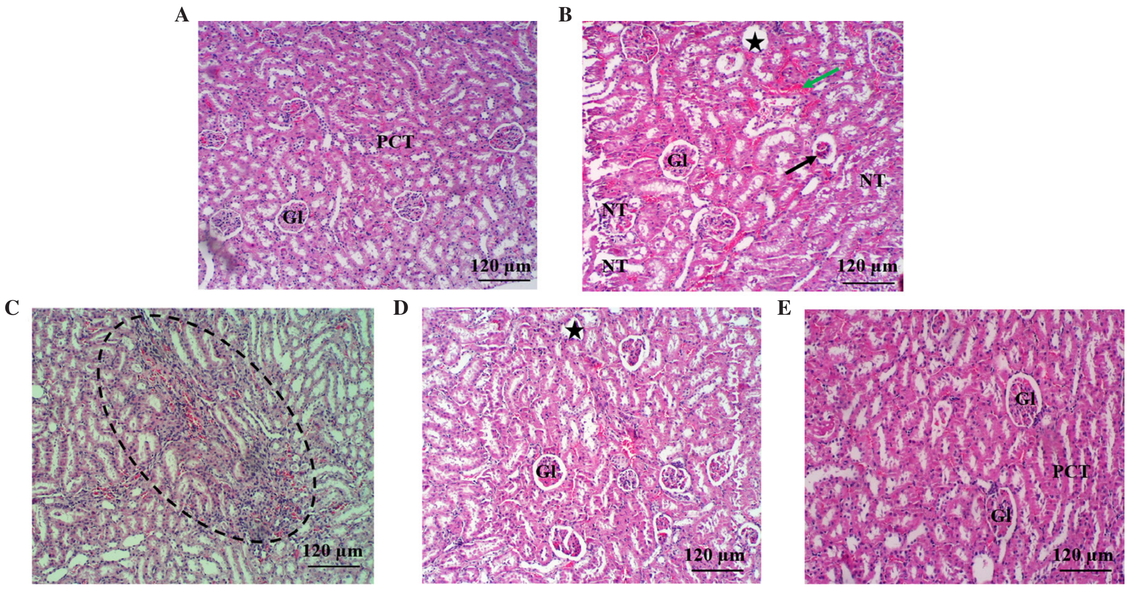

Figure 6. Histological micrographs of renal tissues in experimental groups: (A) Normal, (B) CP, (C) CP + 10 mg/kg BVZnONPs, (D) CP + 20 mg/kg BVZnONPs, and (E) 20 mg/kg BVZnONPs. Black stars: cystic changes; Green arrow: hyperemia; Black arrow: necrotic glomerulus; NT: necrotic tubules; Black dashed-line ellipse: lymphocytic infiltration (H&E staining).

of renal structures in the cortex and medulla. In the CP group, the most changes included hyperemia, congestion, tubule necrosis, cystic changes, and lymphocytic infiltration. These histopathological changes were considerably improved in the treated groups. Moreover, the histological structure of the kidney in the group treated with BVZnONPs alone was normal (Figure 6). This indicated that BVZnONPs have no adverse effects on renal structures.

3.7. Radionuclide scan

Qualitative analysis of the SPECT images showed that CP could impair blood circulation in the renal cortex. This alteration was improved in the treated group and 10 mg/kg of BVZnONPs was better than that in the group treated with 20 mg/kg of BVZnONPs. The SPECT image of the BVZnONPs alone group was almost like the control group image (Figure 7).

4. Discussion

According to this study, CP at 100 mg/kg for 28 d significantly reduced the serum levels of antioxidant enzymes, including CAT, SOD, and GPx, as well as increased renal biochemical parameters Cr and BUN. These observations are in agreement with previous studies that investigated CP toxicity[22–28]. These adverse effects are mediated by the Bax/Caspase-3, 6, p53/cytochrome C, and NF-κB/MAPK signaling pathways[23]. Besides, CP also induced the expression of the apoptotic protein p53 and inhibited the expression of the anti-apoptotic protein Bcl-2. Stereological analysis indicated that CP-induced toxicity resulted in the shrinkage of renal tubules and the replacement of functional kidney tissue with degenerated tissue, leading to a decrease in the overall volume of the kidneys, renal tubules, and glomeruli. This finding is in agreement with the results reported by El Kiki *et al*.[29].

This study demonstrates that BVZnONPs provide a dose-dependent protective effect against nephrotoxicity induced by CP, with the most pronounced effect noted at a dosage of 20 mg/kg. The protective mechanism of BVZnONPs operates through various pathways. These nanoparticles are rich in several polyphenolic compounds, particularly flavonoids, which exert diverse effects. These compounds not only bolster the efficacy of chemotherapy agents in targeting cancer cells but also protect the function and integrity of parenchymal cells from oxidative stress, inflammation, and apoptosis induced by chemotherapy. Additionally, berberine showcased a protective effect against kidney damage caused by CP by lowering serum concentrations of BUN and Cr, while simultaneously elevating levels of antioxidant enzymes such as GPx, GSH, SOD, and CAT[30]. Berberine has been shown to offer protection against gentamicin-induced nephrotoxicity in mice due to its antioxidant, anti-apoptotic, and anti-inflammatory properties. Research by Adil *et al*. indicated that berberine lowers lipid peroxidation in kidney cells by boosting overall antioxidant capacity and enhancing anti-inflammatory effects, as well as increasing the activity of antioxidant enzymes such as CAT and SOD. This action reduces the production of malondialdehyde and free radicals like NO, thereby safeguarding the normal structure and function of the kidneys, which in turn leads to improved kidney function markers such as BUN and Cr levels[31]. Furthermore, berberine has been documented to mitigate CP-induced nephrotoxicity in mice by enhancing antioxidant capacity and decreasing oxidative stress markers in renal tissue[32]. In research of Gholampour *et al*, the hydroalcoholic extract of barberry root, along with its active component berberine, demonstrated protective effects

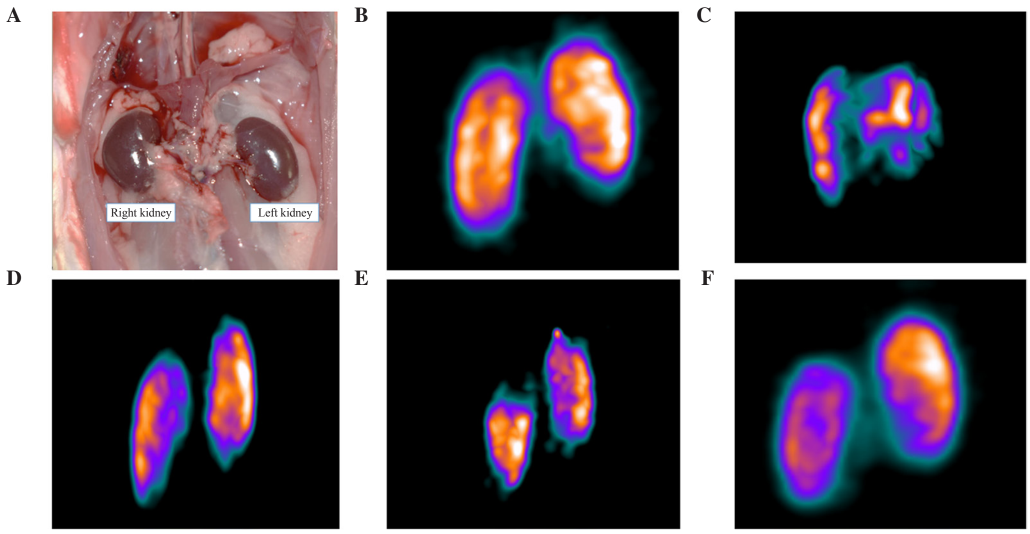

Figure 7. Renal scintigraphy images of the animals in the control and treated groups. (A) Topographic position of the right and left kidney, (B) Normal, (C) CP, (D) CP + 10 mg/kg BVZnONPs, (E) CP + 20 mg/kg BVZnONPs, and (F) 20 mg/kg BVZnONPs.

on the structure and function of both the kidneys and liver in the context of cisplatin toxicity through its anti-inflammatory and anti-apoptotic actions[33].

Besides, the current study shows that CP treatment promoted p53 expression and apoptosis in renal cells in both the central and cortical areas of the kidneys. However, 10 and 20 mg/kg of BVZnONPs were able to prevent apoptosis in the tubular and glomerular cells by inhibiting p53 expression and increasing Bcl-2 expression.

Liquid chromatography-tandem mass spectrometry (LC-MS/MS) analysis of barberry has demonstrated a significant presence of polyphenolic compounds, including 3-caffeoylquinic acid, protocatechuic acid, and 5-caffeoylquinic acid, as well as several flavonoid glycosides such as eleutheroside E, rutin, isoquercitrin, berberine, luteoloside, narcissoside, naringenin-7-glucoside, isorhamnetin-3-glucoside, afzelin, and quercitrin. The antioxidant, anti-inflammatory, and anti-apoptotic properties of barberry are attributed to these bioactive compounds[34]. According to Rafiee *et al.*, barberry extract provided protective effects against the toxic impact of carbon tetrachloride on the testes of Wistar rats by enhancing serum CAT activity and decreasing malondialdehyde levels in testicular tissue, thereby maintaining the structure and function of the testes[35]. A similar research examining the protective benefits of barberry extract on brain tissue in mice subjected to the toxic agent diazinon indicated that the extract boosted the activity of antioxidant enzymes such as GPx, GSH, SOD, and CAT, which resulted in enhanced behavioral performance and improved brain structure[36]. Berberine, 8%-12% of the plant extract has been identified as having protective properties against oxidative damage across various tissues. This compound has been utilized in the treatment of several kidney-related conditions such as diabetic nephropathy, chemotherapy-induced nephropathy, toxicity from heavy metals and nonsteroidal anti-inflammatory drugs, renal fibrosis, renal ischemia, kidney stones, and other forms of renal toxicity[37]. Gholampour and Keikha explored berberine's protective effects against kidney toxicity induced by ferrous sulfate, revealing that berberine enhances the activities of SOD and CAT by boosting total antioxidant capacity, thus safeguarding renal tubules and glomeruli from toxic damage[38]. Additionally, other compounds found in barberry also exhibit protective effects against various urinary system disorders, particularly oxidative, inflammatory, and apoptotic damage related to the kidneys. For instance, Abdel-Raheem *et al*. demonstrated that quercetin protects against oxidative and inflammatory kidney damage caused by gentamicin in rats[39]. Similarly, Almaghrabi highlighted quercetin's protective role against cisplatin-induced kidney damage in rats[40]. Numerous studies have emphasized quercetin's capacity to protect kidney structure and function from oxidative damage inflicted by heavy metals such as lead and cadmium, chemotherapy agents like CP and doxorubicin, and pollutants including carbon tetrachloride[41,42]. Presently, there is a growing focus on the development of nanoparticles, which are synthesized compounds and plant extracts reduced to nano dimensions, owing to their biodegradable, targeted, non-toxic, antimicrobial, and cost-effective characteristics. Metal nanoparticles, particularly those derived from barberry plant extract, enhance the absorption of a variety of organic and inorganic substances, augment stability and shelf life, and act as effective carriers for targeted drug delivery, thereby minimizing the therapeutic doses required.

In this study, BVZnONPs were employed to address renal complications following CP administration. The findings demonstrated that serum markers indicative of kidney function (Cr and BUN) were lower in the treatment groups compared to the CP-only group. Furthermore, the antioxidant properties of BVZnONPs contributed to reducing levels of free radicals (nitric oxide) and boosting the activity of GPx, SOD, and CAT. Immunohistochemical analysis revealed enhanced expression of the anti-apoptotic protein Bcl-2 and diminished expression of the apoptotic protein p53. However, assessments of kidney volume and its various substructures across different groups indicated that 10 and 20 mg/kg of BVZnONPs did not completely restore kidney volume to the normal levels; this may be due to the 28-day treatment duration. Considering the significant reduction in kidney volume resulting from CP, an extended treatment duration might be necessary to fully reverse these severe alterations and optimize the advantageous effects of BVZnONPs on cellular and tissue health.

Some limitations should be considered regarding the present work on the reno-protective effects of BVZnONPs. Initially, we used two different doses of BVZnONPs. More different doses should be examined to achieve better safety and protection. Furthermore, the study focused on apoptosis, oxidative stress, and stereological alterations in the renal tissue, however, other relevant mechanisms such as anti-inflammatory parameters could be evaluated. The other limitations of this study included duration of treatment which can be effective on the obtained results.

In conclusion, this study demonstrates that BVZnONPs could ameliorate effects of CP-induced nephrotoxicity. BVZnONPs decreased Cr and BUN, improved antioxidant enzymes, and decreased apoptosis in CP-injected rats. Therefore, flavonoids may be potentially pharmacological compounds for the prevention of CP-induced renal injury and perhaps other complications, warranting further examinations to precisely determine the underlying mechanism mediating the protective effects of BVZnONPs against CP-related renal tissue damage.

Conflict of interest statement

The authors declare that there is no conflict of interest.

Funding

The authors received no extramural funding for the study.

Data availability statement

The data supporting the findings of this study are available from the corresponding author upon request.

Authors' contributions

RM contributed to animal handling, treatment, and imaging procedures. NG contributed to writing the draft, conceptualization, and supervising the project. HC conducted laboratory tests, and MAB contributed to writing the draft and performing statistical analysis.

References

[1] Desai RJ, Kazarov CL, Wong A, Kane-Gill SL. Kidney damage and stress biomarkers for early identification of drug-induced kidney injury: A systematic review. *Drug Saf* 2022; **45**(8): 839-852.

[2] Kalantar-Zadeh K, Jafar TH, Nitsch D, Neuen BL, Perkovic V. Chronic kidney disease. *Lancet* 2021; **398**(10302): 786-802.

[3] Yin Q, Xiong H. Chemotherapy-induced nephrotoxicity was improved by crocin in mouse model. *Eur J Histochem* 2022; **66**(4): 3541.

[4] Ayza MA, Zewdie KA, Yigzaw EF, Ayele SG, Tesfaye BA, Tafere GG, et al. Potential protective effects of antioxidants against cyclophosphamide-induced nephrotoxicity. *Int J Nephrol* 2022; **2022**(1): 5096825.

[5] Qaed E, Almaamari A, Alyafeai E, Sultan M, Aldahmash W, Mahyoub MA, et al. Phosphocreatine attenuates doxorubicin-induced nephrotoxicity through inhibition of apoptosis and restore mitochondrial function *via* activation of Nrf2 and PGC-1α pathways. *Chem Biol Interact* 2024; **400**. doi: 10.1016/j.cbi.2024.111147.

[6] Ayza MA, Zewdie KA, Tesfaye BA, Wondafrash DZ, Berhe AH. The role of antioxidants in ameliorating cyclophosphamide-induced cardiotoxicity. *Oxid Med Cell Longev* 2020; **2020**(1). doi: 10.1155/2020/4965171.

[7] El-Shabrawy M, Mishriki A, Attia H, Emad Aboulhoda B, Emam M, Wanas H. Protective effect of tolvaptan against cyclophosphamide-induced nephrotoxicity in rat models. *Pharmacol Res Perspect* 2020; **8**(5): e00659.

[8] Özatik FY, Özatik O, Tekşen Y, Koçak H, Arı NS, Ünel ÇÇ. Dose-dependent effect of hydrogen sulfide in cyclophosphamide-induced hepatotoxicity in rats. *Turk J Gastroenterol* 2023; **34**(6): 626-634.

[9] El Kiki SM, Omran MM, Mansour HH, Hasan HF. Metformin and/or low dose radiation reduces cardiotoxicity and apoptosis induced by cyclophosphamide through SIRT-1/SOD and BAX/Bcl-2 pathways in rats. *Mol Biol Rep* 2020; **47**: 5115-5126.

[10] Khoshandam A, Imenshahidi M, Hosseinzadeh H. Pharmacokinetic of berberine, the main constituent of *Berberis vulgaris* L.: A comprehensive review. *Phytother Res* 2022; **36**(11): 4063-4079.

[11] Shakeri F, Kiani S, Rahimi G, Boskabady MH. Anti-inflammatory, antioxidant, and immunomodulatory effects of *Berberis vulgaris* and its constituent berberine, experimental and clinical, a review. *Phytother Res* 2024; **38**(4): 1882-1902.

[12] Hallajzadeh J, Maleki Dana P, Mobini M, Asemi Z, Mansournia MA, Sharifi M, et al. Targeting of oncogenic signaling pathways by berberine for treatment of colorectal cancer. *Med Oncol* 2020; **37**(6): 49. doi: 10.1007/s12032-020-01367-9.

[13] Derakhshani E, Asri M, Naghizadeh A. Plant-based green synthesis of copper oxide nanoparticles using Berberis vulgaris leaf extract: An update on their applications in antibacterial activity. *Bionanoscience* 2023; **13**(1): 212-218.

[14] Salayová A, Bedlovičová Z, Daneu N, Baláž M, Lukáčová Bujňáková Z, Balážová Ľ, et al. Green synthesis of silver nanoparticles with antibacterial activity using various medicinal plant extracts: Morphology and antibacterial efficacy. *Nanomater* 2021; **11**(4). doi: 10.3390/nano11041005.

[15] Marumo A, Omori I, Tara S, Otsuka Y, Konuma R, Adachi H, et al. Cyclophosphamide-induced cardiotoxicity at conditioning for allogeneic hematopoietic stem cell transplantation would occur among the patients treated with 120 mg/kg or less. *Asian Pac J Clin Oncol* 2022; **18**(5): e507-e514.

[16] Akbaribazm M, Goodarzi N, Rahimi M, Naseri L, Khazaei M. Anti-inflammatory, anti-oxidative and anti-apoptotic effects of *Heracleum persicum* L. extract on rats with gentamicin-induced nephrotoxicity. *Asian Pac J Trop Biomed* 2021; **11**(2): 47-58.

[17] Akbari M, Goodarzi N, Tavafi M. Stereological assessment of normal *Persian squirrels* (*Sciurus anomalus*) kidney. *Anat Sci Int* 2017; **92**: 267-274.

[18] Zangeneh MM, Goodarzi N, Zangeneh A, Tahvilian R, Najafi F. Amelioration of renal structural changes in STZ-induced diabetic mice with ethanolic extract of *Allium saralicum* RM Fritsch. *Comp Clin Pathol* 2018; **27**: 861-867.

[19] Bazm MA, Khazaei M, Ghanbari E, Naseri L. Protective effect of *Vaccinium arctostaphylos* L. fruit extract on gentamicin-induced nephrotoxicity in rats. *J Comp Pathol* 2018; **27**: 1327-1334.

[20] Qi R, Wang J, Jiang Y, Qiu Y, Xu M, Rong R, et al. Snai1-induced partial epithelial-mesenchymal transition orchestrates p53-p21-mediated G_2/M arrest in the progression of renal fibrosis *via* NF-κB-mediated inflammation. *Cell Death Dis* 2021; **12**(1): 44. doi: 10.1038/s41419-020-03322-y.

[21] El-Serafi I, Steele S. Cyclophosphamide pharmacogenomic variation in cancer treatment and its effect on bioactivation and pharmacokinetics. *Adv Pharmacol Pharm Sci* 2024; **2024**(1): 4862706.

[22] Ayza MA, Zewdie KA, Yigzaw EF, Ayele SG, Tesfaye BA, Tafere GG, et al. Potential protective effects of antioxidants against cyclophosphamide-induced nephrotoxicity. *Int J Nephrol* 2022; **2022**(1). doi: 10.1155/2022/5096825.

[23]Ou Z, Zhu L, Huang C, Ma C, Kong L, Lin X, et al. Betulinic acid attenuates cyclophosphamide-induced intestinal mucosa injury by inhibiting the NF-κB/MAPK signaling pathways and activating the Nrf2 signaling pathway. *Ecotoxicol Environ Saf* 2021; **225**. doi: 10.1016/j.ecoenv.2021.112746.

[24]Abulyazid I, Abd Elhalim SA, Sharada HM, Aboulthana WM, Abd Elhalim ST. Hepatoprotective effect of carob pods extract (*Ceratonia siliqua* L.) against cyclophosphamide induced alterations in rats. *Int J Curr Pharm Rev Res* 2017; **8**(2): 149-162.

[25]Goudarzi M, Khodayar MJ, Hosseini Tabatabaei SMT, Ghaznavi H, Fatemi I, Mehrzadi S. Pretreatment with melatonin protects against cyclophosphamide-induced oxidative stress and renal damage in mice. *Fundam Clin Pharmacol* 2017; **31**(6): 625-635.

[26]Temel Y, Kucukler S, Yıldırım S, Caglayan C, Kandemir FM. Protective effect of chrysin on cyclophosphamide-induced hepatotoxicity and nephrotoxicity *via* the inhibition of oxidative stress, inflammation, and apoptosis. *Naunyn–Schmiedeberg's Arch Pharmacol* 2020; **393**: 325-337.

[27]Chen L, Xiong X, Hou X, Wei H, Zhai J, Xia T, et al. Wuzhi capsule regulates chloroacetaldehyde pharmacokinetics behaviour and alleviates high-dose cyclophosphamide-induced nephrotoxicity and neurotoxicity in rats. *Basic Clin Pharmacol Toxicol* 2019; **125**(2): 142-151.

[28]Hammodi HZ, Al-Shawi NN. Protective effect of daidzein on ifosfamide-induced neurotoxicity *via* improving some selected oxidative stress parameters in male rats. *Iraqi J Pharm Sci* 2023; **32**(Suppl): 53-60.

[29]El Kiki SM, Omran MM, Mansour HH, Hasan HF. Metformin and/or low dose radiation reduces cardiotoxicity and apoptosis induced by cyclophosphamide through SIRT-1/SOD and BAX/Bcl-2 pathways in rats. *Mol Biol Rep* 2020; **47**: 5115-5126.

[30]Mombeini MA, Kalantar H, Sadeghi E, Goudarzi M, Khalili H, Kalantar M. Protective effects of berberine as a natural antioxidant and anti-inflammatory agent against nephrotoxicity induced by cyclophosphamide in mice. *Naunyn–Schmiedeberg's Arch Pharmacol* 2022; **395**(2): 187-194.

[31]Adil M, Kandhare AD, Dalvi G, Ghosh P, Venkata S, Raygude KS, et al. Ameliorative effect of berberine against gentamicin-induced nephrotoxicity in rats via attenuation of oxidative stress, inflammation, apoptosis and mitochondrial dysfunction. *Renal Fail* 2016; **38**(6): 996-1006.

[32]Allameh H, Fatemi I, Malayeri AR, Nesari A, Mehrzadi S, Goudarzi M. Pretreatment with berberine protects against cisplatin-induced renal injury in male Wistar rats. *Naunyn–Schmiedeberg's Arch Pharmacol* 2020; **393**: 1825-1833.

[33]Gholampour F, Masoudi R, Khaledi M, Rooyeh MM, Farzad SH, Ataellahi F, et al. Berberis integerrima hydro-alcoholic root extract and its constituent berberine protect against cisplatin-induced nephro-and hepato-toxicity. *Am J Med Sci* 2022; **364**(1): 76-87.

[34]Och A, Olech M, Bąk K, Kanak S, Cwener A, Cieśla M, et al. Evaluation of the antioxidant and anti-lipoxygenase activity of *Berberis vulgaris* L. leaves, fruits, and stem and their LC MS/MS polyphenolic profile. *Antioxidants* 2023; **12**(7). doi: 10.3390/antiox12071467.

[35]Rafiee F, Nejati V, Heidari R, Ashraf H. Protective effect of methanolic extract of *Berberis integerrima* Bunge. root on carbon tetrachloride-induced testicular injury in Wistar rats. *Int J Reprod Biomed* 2016; **14**(2): 133-140.

[36]Sonei A, Fazelipour S, Kanaani L, Jahromy MH. Protective effects of *Berberis vulgaris* on diazinon-induced brain damage in young male mice. *Prev Nutr Food Sci* 2020; **25**(1): 65-70.

[37]Hassanein EH, Ibrahim IM, Abd-Alhameed EK, Mohamed NM, Ross SA. Protective effects of berberine on various kidney diseases: Emphasis on the promising effects and the underlined molecular mechanisms. *Life Sci* 2022; **306**. doi: 10.1016/j.lfs.2022.120697.

[38]Gholampour F, Keikha S. Berberine protects the liver and kidney against functional disorders and histological damages induced by ferrous sulfate. *Iran J Basic Med Sci* 2018; **21**(5): 476-482.

[39]Abdel-Raheem IT, Abdel-Ghany AA, Mohamed GA. Protective effect of quercetin against gentamicin-induced nephrotoxicity in rats. *Biol Pharm Bull* 2009; **32**(1): 61-67.

[40]Almaghrabi OA. Molecular and biochemical investigations on the effect of quercetin on oxidative stress induced by cisplatin in rat kidney. *Saudi J Biol Sci* 2015; **22**(2): 227-231.

[41]Morales AI, Vicente-Sánchez C, Jerkic M, Santiago JM, Sánchez-González PD, Pérez-Barriocanal F, et al. Effect of quercetin on metallothionein, nitric oxide synthases and cyclooxygenase-2 expression on experimental chronic cadmium nephrotoxicity in rats. *Toxicol Appl Pharmacol* 2006; **210**(1-2): 128-135.

[42]Bakir A, Suat E, Yüksek S, Gokhan OTO. The protective effect of *Rheum Ribes* L. and quercetin on protein carbonyl levels against carbon tetrachloride-induced liver and kidney damage in the rats. *Clin Exp Health Sci* 2022; **12**(3): 587-593.

Publisher's note

The Publisher of the *Journal* remains neutral with regard to jurisdictional claims in published maps and institutional affiliations.

Edited by Tan BJ, Liang Q